STRUCTURAL RESPONSE OF A REINFORCED CONCRETE SPECIMEN SUBJECTED TO BLAST LOADING

КОНСТРУКТИВНА РЕАКЦИЯ НА ЕЛЕМЕНТ ОТ УСИЛЕН БЕТОН ПОДЛОЖЕН НА ВЗРИВНО НАТОВАРВАНЕ

M.Sc. Petkov Y[1] , Assoc. Prof. M.Sc. Ganev R. PhD. [1], Prof. MSc. Lilov I. PhD[2]
Higher School of Civil Engineering (VSU) "L. Karavelov" – Sofia, Bulgaria[1]
National Military University, Veliko Turnovo, Bulgaria[2]

petkov.yordan@gmail.com

Abstract: *Field tests of fiber-reinforced concrete (FRC) and reinforced concrete specimens were performed by research team from Faculty of Civil Engineering, Czech Technical University in Prague, Czech Republic in cooperation with University and the Czech Army corps in the military training area Boletice. The test were performed using real scale reinforced concrete precast slabs (6 x 1.5 x 0.3m) with varying fiber type, fiber strength, fiber content and concrete strength class. TNT charges of 25kg placed at distance from the slab for better simulation of real in-situ conditions. The paper presents conclusions from sets of tests from 2016 and three previous in 2010, 2011 and 2013. Eleven specimens were tested in total. Two specimens were without fibres and had different concrete strength. Polypropylene fibres (PP) with length 50mm and strength of 600MPa and steel fibers (FE) with low ductility 25mm long and strength 400MPa were added in different content (0.5% and 1%) to the other nine specimens.*

KEYWORDS: BLAST LOAD, RC STRUCTURES, STEEL FIBRES, POLYPROPYLEN FIBRES, EXPLOSION, BLAST WAVE

1. Introduction

The rising threat from terrorist attacks using different explosive materials is a significant threat to the modern society. The biggest damages are caused by the blast load on objects from critical infrastructure. The report presents the results from experiments of a method of monitoring the shock wave propagation and spall formation using a high speed framing camera. The use of a high speed camera for full scale concrete blast loading experiments is frequently mentioned in the literature, but small number of articles provides useful results of such kind recordings.

Due to improved ductility, fiber-reinforced concrete (FRC) shows better performance under blast and impact loading compared to conventionally reinforced concrete, as mentioned in many sources. The experiments from year 2016 determine blast performance of FRC with low strength and low ductility steel fibers (strength 400 MPa).

2. Setup of the experiments

Dimensions of the specimens were designed in real scale of a small span bridge as concrete slabs, 6m long, 1.5m wide and 0.3m thick.

The slabs were placed on timber posts and the soil under the slabs was removed; a channel 10m in length and 2.3m in depth (except 1.5m in test 1) was excavated under the slabs in order to allow observation of the soffit.

The 25kg TNT charges were built up using standard military 200g TNT charges. The charges were placed on steel holders in the middle of the slabs. The holders provided a 450mm stand-off distance from the slab for better simulation of real in-situ conditions. This value was chosen as the most usual height of a car trunk. The setup of the experiment is shown in fig. 1.

Fig. 1 *Layout of the experiment*.

3. Instrumentation

The early stages of spall formation were observed on the soffit using angled mirrors which were placed under the concrete specimens. Another mirror was placed in front of the cameras in order to allow indirect observation without the risk of camera damage by fragments.

The experiments were captured using a NAC Memrecam GX3 high speed movie camera and IVV UHSi 12/24 ultra-high speed framing camera, the former being intended for expected spall formation while the latter for crack growth observations.

Sigma 70–300mm f/4–5.6, Samyang 800mm f/8, and Samyang 85mm f/1.4 lenses were mounted on the cameras. The aperture and gain were set to maximum values. The frame rates, single frame exposure times, and lens types are shown in Table 1. The view of the cameras can be seen in fig. 2.

Table 1: *Camera settings. *Note: [1]Lens types: A - Sigma 70-300 mm; B – Samyang 800 mm; C – Samyang 85 mm*

Test №	Lens[1]	Exposure time [μs]	Frame rate [s^{-1}]	Lens[1]	Exposure time [μs]	Frame rate [s^{-1}]
1	C	64	15000	A	2	50000
2	C	50	15000	A	2	10000
3	A	50	15000	B	5	10000
4	A	20	20000	C	5	10000
5	A	50	15000	C	5	10000

Fig. 2 *Camera view*.

4. Results and discussions

The process of blast loading of concrete has the following time schedule. The detonation of the main charge generates an expanding cloud of gases led by a strong shock wave which approaches the concrete specimen. The shock wave partially reflects back from the specimen surface. The compressive stress at the top surface of the specimen can cause local crushing of concrete or a shear failure of the specimen (puncture by shear-punching behavior). The other part of the shock wave passes through to the bottom side of the specimen, where it reflects again, interfering with the release part itself. In this time, cracks develop on the soffit and the spall begins to form. Part of the shockwave again passes through the interface, creating an air shock wave under the specimen. This air shock wave is combined with a shock wave which overflows the test specimen from the side. The air shock wave is later followed by flying spall debris.

Results of monitoring the blast wave propagation, which were obtained from the Memrecam records, can be seen in Table 2 and fig. 3–6. The first cracks are visible on the soffit at about 0.3ms after the main charge detonation according to test 4, but they probably formed earlier. The average spall debris velocity was 120m.s^{-1}. In test 1, the air shock wave velocity under the specimen as determined from the movie reached 1150m.s^{-1} while it was only 480m.s^{-1} and 600m.s^{-1} in tests 2 and 5, respectively.

Table 2: *Monitoring of blast wave propagation.*

Test №	Test №1		Test №2		Test №3		Test №4		Test №5	
	frame	time [ms]	frame	time [ms]	frame	time [ms]	frame	time [ms]	frame	time [ms]
Detonation of the auxiliary charge	0	1.93	0	2.13	0	1.93	0	1.65	0	2.00
Detonation of the main charge	29	0	32	0	29	0	33	0	30	0
Crack development on the soffit	42	0.85	44	0.80	34	0.33	39	0.30	37	0.47
Shock wave arrive to the ground	59	2.00	86	3.60	94	4.33	122	4.45	85	3.67
Spall debris arrive to the mirror upper edge	---	---	183	10.07	---	---	---	---	173	9.53
Shock wave arrive to the second mirror	---	---	1101	71.27	---	---	1445	70.60	1080	70

Fig. 3 *Spalling just started on the soffit (test 5, t = 0.67 ms).*

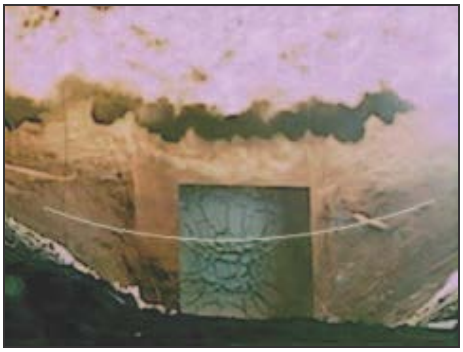

Fig. 4 *Air shock wave passes along the mirror (highlighted by the white line, test 5; t = 2.8 ms).*

Fig. 5 *Extended damage of the soffit (test 4; t = 2.85 ms).*

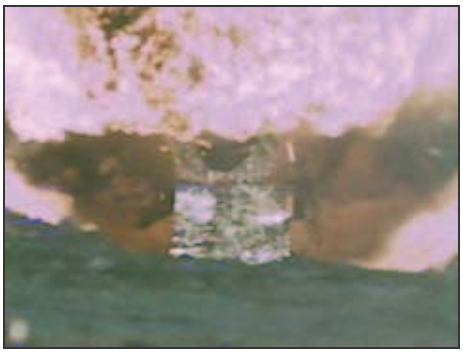

Fig. 6 *The flying spall debris reach the upper edge of the mirror (test 2;t = 10 ms).*

5. Numerical modelling of the specimen response

LS-DYNA solver was used for computing the response of the specimen to the adjacent blast. The setup of the numerical model was adapted from previous experiments.

A numerical model was successfully calibrated to describe the behavior of concrete slabs subjected to blast loading and the corresponding damage.

The camera instrumentation confirmed some numerical model expectations. The overpressure wave arrived at the top surface of the specimen at t=0.2ms in the numerical model. After the rebound of the overpressure wave from the soffit of the specimen, the first elements started to erode (t=0.4ms). fig. 7 shows the contours of normal stress in time t=0.3 ms.

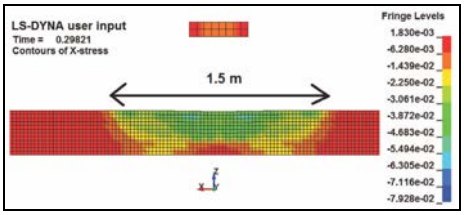

Fig. 7 *Normal stress – t=0.3ms*

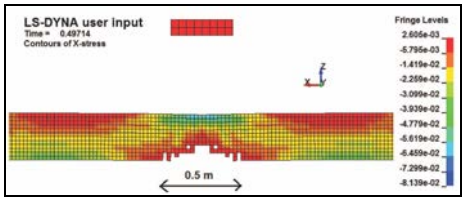

Fig. 8 *contours of normal stress in time t = 0.5 ms – eroded elements on the soffit*

The extend crack development is an indicator of the extent of damage of the concrete. Material model MAT159_CSCM used in LS-DYNA solver for concrete elements have another indicator for damage; the plastic strain value. If the plastic strain indicator overpasses the setting value, concrete elements erode.

Differentiating between numerical simulation and real behavior of concrete is in the eroding elements in the model and inertia of concrete in real conditions. The concrete element has its own static inertia and does not erode in the same time in real behavior and numerical simulation. The shape and the size of a plastic strain pattern is the decisive parameter for the modeling and experiments' agreement consideration.

For detailed concrete loss of weight research, the 3D models of concrete slabs were created. The crack, puncture and spalling patterns were made in every concrete layer in accordance to a known depth. The connection of separated layer patterns brought the 3D model of the concrete slab (fig 9).

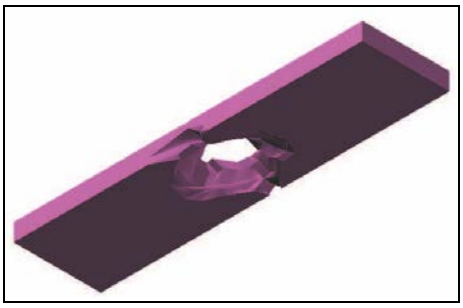

Fig. 9 *3D model of damaged specimen*

6. Conclusions

The observation of real scale blast loading experiments using high speed cameras was performed according to the experiment request.

The spall formation process on the soffit and blast waves under the specimen were captured using a Memrecam movie camera, allowing the air shock wave and spall debris velocities to be estimated. The attempt to catch the foremost crack growth on the soffit using the UHSi camera was not successful due to insufficient illumination of the target. The model of spall formation was created using LS-DYNA solver.

For the next experiments, concrete shielding panels for more efficient fireball elimination and also an improved triggering system are being designed. LS-DYNA solver was used for computing the response of the specimen to the adjacent blast.

7. Literature

[1] Foglar M., Kovar M., Conclusions from experimental testing of blast resistance of FRC and RC bridgedecks, International Journal of Impact Engineering, Volume 59, September 2013, Pages 18-28, ISSN 0734-743X

[2] Wu C., Oehlers D.J., Rebentrost M., Leach J., Whittaker A.S., Blast testing of ultra-high performance fibre and FRP-retrofittedconcrete slabs, Engineering Structures, Volume 31, April 2009, Pages 2060-2069, ISSN 0141-0296

[3] Coughlin A.M., Musselman E.S., Schokker A.J., Linzell D.G., Behavior of portable fiber reinforced concrete vehicle barrierssubject to blasts from contact charges, International Journal of Impact Engineering, Volume 37, 2010, Pages 521-529, ISSN 0734-743X

[4] Millard S.G., Molyneaux T.C.K., Barnett S.J., Gao X., Dynamic enhancement of blast-resistant ultra-high performance fibre-reinforced concrete under flexural and shear loading, International Journal of Impact Engineering, Volume 37, Issue 4, April 2010, Pages 405-413, ISSN 0734-743X

[5] Kovar M., Foglar M., Hajek R., The blast performance of real-scale reinforced concrete specimens with varying fibre type and content, Structure under shock and impact, XIII, Volume 141, Pages 159-169, ISSN 1743-3509.

[6] Hajek R., Foglar M., Kohoutkova A., Recent development in blast performance of fiber-reinforced concrete, Fibre conference 2017, Materials Science and Engineering, Pages 246-256, ISSN 1743-3509

[7] Stohr J, Hajek R, Foglar M 2015 Blast performance of reduced scale reinforced concrete specimens Civil-Comp Proc. 108